Do clinical, histological or immunohistochemical primary tumour characteristics translate into different 18F-FDG PET/CT volumetric and heterogeneity features in stage II/III breast cancer?

David Groheux, Mohamed Majdoub, Florent Tixier, Catherine Cheze Le Rest, Antoine Martineau, Pascal Merlet, Marc Espié, Anne de Roquancourt, Elif Hindié, Mathieu Hatt, et al.

Do clinical, histological or immunohistochemical primary tumor characteristics translate into different ^{18}FDG-PET/CT volumetric and heterogeneity features in stage II-III breast cancer?

David Groheux[1], Mohamed Majdoub[2], Florent Tixier[2,3], Catherine Cheze Le Rest[3,2], Antoine Martineau[1], Pascal Merlet[1], Marc Espié[4], Anne de Roquancourt[5], Elif Hindié[6], Mathieu Hatt[2*], Dimitris Visvikis[2*]

[*] equally contributed

[1] Department of Nuclear Medicine, Saint-Louis Hospital, Paris, France.

[2] INSERM, UMR 1101 LaTIM, Brest, France.

[3] Department of Nuclear Medicine, Milétrie Hospital, Poitiers, France.

[4] Breast Diseases Unit and Department of Medical Oncology, Saint-Louis Hospital, Paris, France.

[5] Department of Pathology, Saint-Louis Hospital, Paris, France.

[6] Department of Nuclear Medicine, CHU Bordeaux, University of Bordeaux, France.

Corresponding author: M. Hatt,
INSERM, UMR 1101, LaTIM
CHRU Morvan, 2 avenue Foch
29609, Brest, France
Tel: +33(0)2.98.01.81.11
Fax: +33(0)2.98.01.81.24
E-mail: hatt@univ-brest.fr

Wordcount: ~5830

Abstract:

Purpose: This retrospective study aimed at determining if some features of baseline ^{18}FDG-PET images, including volume and heterogeneity, reflect clinical, histological or immunohistochemical characteristics in stage II and III breast cancer (BC) patients.

Methods: 171 stage II-III BC patients treated consecutively in Saint-Louis hospital and prospectively recruited were included in the present retrospective analysis. Primary tumor volumes were semi-automatically delineated on pre-treatment ^{18}FDG-PET images. Extracted parameters included SUV_{max}, SUV_{mean}, Metabolically Active Tumor Volume (MATV), Total Lesion Glycolysis (TLG) and heterogeneity quantification using the area under the curve of the cumulative histogram and textural features. Association between clinical/histopathological characteristics and ^{18}FDG-PET features was assessed using one-way analysis of variance. Area Under the ROC Curves (AUC) was used to quantify the discriminative power of features significantly associated with clinical/histopathological characteristics.

Results: T3 tumors (>5cm) exhibited higher textural heterogeneity in ^{18}FDG uptake than T2 tumors (AUC<0.75), whereas SUV_{max} or SUV_{mean}were not significantly different. Invasive ductal carcinoma showed higher SUV_{max} values than invasive lobular carcinoma (p=0.008) but MATV, TLG and textural feature analysis were not discriminative. Grade-3 tumors had higher FDG uptake (AUC=0.779 for SUV_{max} and 0.694 for TLG), and exhibited slightly higher regional heterogeneity (AUC=0.624). Hormone receptor-negative tumors had higher SUV values than Estrogen Receptor (ER) and progesterone receptor positive tumors, while heterogeneity patterns showed only low-level variation according to hormone receptor expression. HER-2 status was not associated with any of the image features. Finally, SUV_{max},

$SUV_{mean}$and TLG significantly differed between 3 phenotypic subgroups (HER2-positive, triple-negative and ER-positive/HER2-negative BCs) but MATV and heterogeneity metrics were not discriminative.

Conclusion: SUV parameters, MATV and textural features present limited correlation with clinical and histopathological features. The 3 main BC subgroups differ in term of SUVs and TLG but not in terms of MATV and heterogeneity. None of the PET-derived metrics offered high discriminative power.

Keywords: ^{18}FDG-PET/CT, heterogeneity, textural features, breast cancer.

Introduction

^{18}F-FluoroDeoxyGlucose(^{18}FDG) Positron Emission Tomography/ Computed Tomography (PET/CT) becomes increasingly important for staging Breast Cancer (BC) patients with large or locally-advanced disease [1,2]. These patients usually receive neoadjuvant treatment (chemotherapy ± targeted therapy or endocrine-therapy), surgery, radiation therapy and sometimes adjuvant systemic treatment. However, BC comprises different phenotypes with different response rates to chemotherapy, different treatment options, and different prognoses [3]. In clinical practice, 3 main entities based on immunohistochemical analysis of the primary tumor biopsy are currently considered: the Estrogen Receptor (ER)-positive/HER2-negative, the HER2-positive and the Triple-Negative BC (TNBC) subgroups[4]. Specific systemic treatments are used in each subgroup. For example, large or locally-advanced HER2-positive BC are treated with neoadjuvant chemotherapy plus trastuzumab. Recent works have shown that dual inhibition of HER2 (trastuzumab+lapatinib or trastuzumab+pertuzumab) improves the pathological complete response rate in this subtype of BC[5]. However, it also involvesstronger side-effects, hence the importance of patient selection to reserve these novel treatments for patients with poor prognosis.

Clinical and pathological BC characteristics are currently used to guide treatment. For examples, patients with lymph nodes involvement have poorer prognosis than patients with no lymph node involvement(N0) and higher grade tumors are more aggressive than lower grade tumors. More recently genetic prognostic tests (*e.g.* oncotype DX in ER-positive tumors) emerged as promising tools to individualize treatment. However there is still room for other prognostic factors and ^{18}FDG-imaging could provide some. It has been shown that high baseline ^{18}FDG uptake

(SUV_{max}) is associated with poor prognostic factors such as the high SBR-grade[6,7] and worse survival [8].

Recently heterogeneity PET derived quantitative measurements emerged also as potential prognostic factors in several cancer types. In BC, results from one recent study suggested that texture analysis might be used, in addition to SUV_{max}, as a new tool to assess invasive BC aggressiveness [9]. Another team reported that heterogeneity was associated with survival in BC patients with Invasive Ductal Carcinoma (IDC)[10].

Our present study included a larger number (171) of consecutive patients with stage II and III BC.It was designed to investigate in detail the relationship between some clinical, histological and immunohistochemical BC prognostics factors and volumetric and heterogeneity PET measurements.

MATERIALS AND METHODS

Study Design

We performed a retrospective analysis of data acquired prospectively in the ASAINT study, which examines the role of ^{18}FDG-PET/CT in patients with stage II-III BC undergoing neoadjuvant chemotherapy in Saint-Louis hospital[1]. The present analysis included 171 consecutive stage II-III BC patients. The first and last included patient underwent imaging on 07/2007 and 04/2013respectively. Patients with distant metastases were not included. Stage I patients received primary surgery with sentinel lymph node biopsy and PET/CT was not performed for these patients. The primary aim was to evaluate the correlations between a large panel of baseline ^{18}FDG-PET imaging-derived features (encompassing volumetric and heterogeneity metrics) and clinical data (*e.g.*, patient age, cTNM classification), histological and

immunohistochemical parameters (*e.g.*, tumor grade, hormone receptor expression) and BC subgroups phenotype (ER-positive/HER2-negative BC, HER2-positive BC and TNBC). A secondary aim was to quantify the discriminative power of features found to be significant.

Tumor Histology and Immunohistochemistry

Core-needle biopsy performed before treatment was used for diagnosis. Tumors were graded using the modified Scarff-Bloom-Richardson system. Tumors were determined to be ER-positive in the presence of moderate or high positivity (2 or 3+) of at least 10% of cells. Progesterone receptor (PR)-positive status was determined according to the same criteria.

Tumors were considered to overexpress c-erbB-2 oncoprotein (HER2-positive) if more than 30% of invasive tumor cells showed definite membrane staining resulting in a so-called fishnet appearance[11]. Control by fluorescence *in situ* hybridization or silver *in situ* hybridization was done for ambiguous cases.

TNBC was defined as ER-negative, PR-negative and HER2-negative. Tumors were subsequently classified into three phenotypes: TNBC, HER2-positive BC and ER-positive/HER2-negative BC.

^{18}FDG-PET/CT Imaging

Blood glucose level had to be <7mmol/L and patients fasted for 6 hours before intravenous injection of 5MBq/Kg of ^{18}FDG, administered in the arm opposite to the breast tumor. Imaging on a Gemini XL PET/CT scanner (germanium oxyorthosilicate-based PET, 16 slice Brilliance CT, Philips Medical systems) started 60min after injection. It was carried out from mid-thigh level to the base of the skull,

with the arms raised. CT data were acquired first (120kV; 100mAs; no contrast-enhancement). PET emission data were acquired in a 3-dimensional mode (2 min/bed position). PET images were reconstructed with the default manufacturer-provided method: 3D row-action maximum likelihood algorithm (4×4×4mm^3 voxels) and CT based attenuation correction, normalized for injected activity and body weight, and subsequently converted into Standardized Uptake Values (SUV), using: [tracer concentration (kBq/mL)] / [injected activity (kBq)/patient body weight (g)].

PET-derived features

For each patient, the primary tumor was identified by a nuclear medicine specialist. Metabolically Active Tumor Volumes (MATVs) of the primary tumors (not the involved lymph nodes) were automatically segmented using the Fuzzy Locally Adaptive Bayesian (FLAB) algorithm previously validated for both homogeneous and heterogeneous uptakes [12,13]including in BC [14]. Total Lesion Glycolysis (TLG) was defined as the product of MATV and SUV_{mean}both obtained through the FLAB delineation. Heterogeneity of the PET uptake within the delineated MATV was quantified through two different methods. Firstly, the Area Under the Curve of the Cumulative Histogram (CH_{AUC}), a method quantifying global tumor heterogeneity [15]. Secondly, five Textural Features (TF) chosen based on previous investigations [16–19], corresponding to the most robust with respect to partial volume effects, segmentation [18], reconstruction settings [20], as well as test-retest physiological reproducibility [17]. All TFs were calculated with a quantization in 64 grey-levels [17–19]. These using a co-occurrence matrix taking into account all 13 directions simultaneously without an averaging step [19] were Entropy (E), Dissimilarity (D),as well asHomogeneity (H) that was included for comparison with a recent study [9].

They quantify local heterogeneity at the scale of a voxel and its neighborhood. TFs calculated using size-zone matrices included High Intensity Large Area Emphasis (HILAE) and Zone Percentage (ZP). They quantify regional heterogeneity based on the respective sizes and intensities of groups of voxels. Figure 1 provides an example of two tumors with different levels of heterogeneity.

Because heterogeneity quantification in PET images using TFs can be confounded by tumor volume effects for small tumor volumes, especially <10cm^3[19,21], we also performed a sub-analysis for MATVs>10cm^3.

Statistical analysis

Statistical analyses were performed using Medcalc^{TM} (MedCalc Software, Belgium).

The feature values were expressed with median ± Standard Deviation (SD) and range (min-max). Correlations between PET features were assessed using Spearman rank coefficients (rho).

The association with each PET feature of clinical, histopathological factors andsubgroups (TNBC, HER2-positive, ER-positive/HER2-negative) was assessed using one-way analysis of variance. For distributions not normally distributed, a log transformation was first applied. For ER, PR and HER2 status, positive cases were compared to negative cases. Tumors of low and intermediate grade (1-2) were compared to high-grade tumors (grade-3). T1 and T2 tumors (clinically estimated at ≤5cm diameter) were compared to T3 tumors (>5cm), excluding T4 from the analysis because of the specificity of T4 staging not based on tumor size. N0 cases were compared to cases with clinical lymph node involvement (N1, N2 or N3). The three main histology types of this series (invasive ductal, lobular, and metaplastic carcinoma) were compared. For each PET feature significantly associated with a

clinical or a histopathological factor or a BC subgroup, its discriminative power was quantified by reporting Areas Under theReceiver Operating Characteristic (ROC)Curve (AUC).

All tests were two-sided and p-values <0.05 were considered statistically significant, with correction for multiple testing being performed using the false discovery rate Benjamini-Hochberg step-up procedure. It consists in declaring positive discoveries at level α (here α=0.05), among the k=1…K tested variables (here K=10) ordered (increasing order) according to their p-values, those ranked above the one satisfying the condition $p(k) \leq k/K \times \alpha$ [22].

RESULTS

Patients' characteristics

Eighty-six patients had stage II and 85 stage III BC. Most patients had IDC (156/171).There were 54 TNBC, 33 HER2-positive and 84 ER-positive/HER2-negative tumors. Other clinical and histopathological factors are provided in table 1. Three patients had a tumor size ≤2cm (T1 tumor), in which ^{18}FDG uptake could be identified with SUV_{max}>2.5. Among the 89 tumors with MATV>10cm^3, there were 33 TNBC, 19 HER2-positive, and 37 ER-positive/HER2-negative tumors.

Correlation between features

Correlation with MATV ranged from |rho|<0.2 for SUV_{max}, SUV_{mean} and CH_{AUC}, to |rho|>0.67 for TFs (except HILAE with rho=0.06): -0.88 for D, 0.79 for E, 0.85 for H and -0.68 for ZP. H was found to be highly correlated with D (rho=0.97) and ZP (rho=0.80). HILAE and CH_{AUC} were also highly correlated (rho=0.93) (supplemental table 1).

Association between clinical factors and PET features

Patient age was not found to be associated with any PET feature (table 2). The median SUV_{max} was 7.6 in women ≤50 y *vs.* 6.9 in women >50 y (p=0.09). T3 tumors exhibited similar levels of ^{18}FDG uptake (SUV_{max} and SUV_{mean}) as T2 tumors. They were nevertheless associated with significantly larger MATV (12.1±15.9 *vs.* 6.5±7.2 cm^3; p<0.001) and TLG (42.7±92.3 *vs.* 22.8±60; p<0.001). They also exhibited higher global heterogeneity (CH_{AUC}, 0.32±0.06*vs.* 0.34±0.05; p=0.018) and higher local and regional heterogeneity (*e.g.* entropy of 7.1±0.35 *vs.* 6.8±0.6; p<0.001). However, the associated AUCs were modest:<0.7 except D and H with 0.733 and 0.730 respectively.

None of the PET-image derived features of the primary breast tumor was associated with absence (N0) or presence (N1-3) of involved lymph nodes.

Association between histological, immunohistochemical factors and PET features

Invasive Lobular Carcinoma (ILC) had significantly lower uptake than IDC (SUV_{max} 3.7±1.2 *vs.* 7.4±5.2; p=0.008) (table 2). SUVs were not significantly different between IDC and metaplastic carcinoma (SUV_{max} 7.4±5.2 *vs.* 6.6±5.3; p=0.75). None of the heterogeneity metrics were significantly associated with histology.

Grade-3 tumors exhibited significantly higher uptake compared to grade-1 and grade-2 tumors (SUV_{max} 9.2±5.4 *vs.* 5.3±3.6; SUV_{mean} 5.1±3.2 *vs.* 3.1±2.0; and TLG 64.8±516.8 *vs.* 25.1±54.7; p<0.001 for each) (figure 2). Grade-3 tumors also exhibited slightly higher regional heterogeneity (HILAE of 927±307 for grade-3 *vs.* 792±233 for grade-1 and grade-2; p=0.012), whereas differences in terms of volume (p=0.034) and local heterogeneity (E, p=0.04) did not reach statistical significance

after correction for multiple testing. *In fine*, the AUCs of associations with grade-3 tumors were 0.779 for SUV_{max} and 0.769 for SUV_{mean}, and <0.7 for TLG and HILAE.

ER-positive and PR-positive tumors were both associated with significantly ($p \leq 0.001$) lower SUVs (SUV_{max} 6.4±3.8 for ER-positive *vs.* 9.0±5.9 for ER-negative and 5.8±3.9 for PR-positive *vs.* 7.7±5.4 for PR-negative). MATVs were significantly smaller ($p<0.03$) in ER-positive (9.2±39.9cm^3 *vs.* 12.4±54.8cm^3 for ER-negative) and in PR-positive tumors (8.2±14.2cm^3 *vs.* 11.9±57.2cm^3 for PR-negative). Lower local heterogeneity (D and H) was seen in the case of hormone-positive BC (table 2). PR-positive tumors also exhibited lower E (6.9±0.6 *vs.* 7.1±0.5, $p=0.025$). Overlaps between ER/PR-positive and negative tumors were very important, with AUCs ≤0.67 (obtained with SUV_{max}).

Only SUV_{max}, SUV_{mean} and TLG were found to be significantly associated ($p \leq 0.001$) with the three BC subgroups: ER-positive/HER2-negative BC, HER2-positive BC and TNBC (figure 3A). TNBC exhibited the highest SUV_{max} (9.8±6.2) compared to HER2-positive (7.0±4.5) and ER-positive/HER2-negative BCs (6.2±3.6). Neither MATV (figure 3B) nor any of the derived heterogeneity quantification metrics (global, regional or local scales) were found to be significantly different among the three BC subgroups, after correction for multiple testing (table 2). Results were similar when restricting the analysis to the 89 patients with MATV>10cm^3, although the statistical significance of SUV_{max} ($p=0.045$) and SUV_{mean} ($p=0.033$) was lost after correction for multiple testing.

Among the three PET features (SUV_{max}, SUV_{mean} and TLG) found to be significantly associated with the 3 BC subgroups, SUV_{max} offered the highest (yet still limited) discriminative power to identify patients with TNBC (0.713) and ER-positive/HER2-negative BC (0.675) (figure 4B, 4C). SUV_{mean} had slightly lower discriminative power,

whereas TLG was least discriminative. Regarding the identification of HER2-positive tumors, none of the PET features had discriminative power (all AUCs ≤0.547) (figure 4A).

DISCUSSION

Recently a growing interest in PET image derived features beyond the usual SUV measurements has emerged in oncology, including volumetric, shape and heterogeneity metrics [16,23], with special reference to the comprehensive quantification of tumor phenotypes or popularly denoted "*radiomics*" [24,25]. It has been recently shown that cancer subgroups could be non-invasively identified using image-based *radiomics* features extracted from dosimetry planning CT images in large cohorts of patients with non-small cell lung cancer and head and neck cancer [24]. Some of these new heterogeneity and shape metrics in ^{18}FDG-PETimages have shown some value in predicting response to therapy or as prognostic factors in several solid tumors such as head and neck [26], esophageal [16] and lung cancer [27,28].

BC is a heterogeneous class of tumors. The various BC subgroups differ in biology profiles, treatment possibilities, and outcomes. We have previously reported that high ^{18}FDG uptake is correlated to histological and biological poor prognostic factors in BC. Notably we found that^{18}FDG uptake was higher in the case of TNBC than in ER-positive tumors [6] and TNBC have poorer prognosis[29].

FDG uptake distribution has been associated with underlying physiopathological characteristics such as vascularization, perfusion, tumor aggressiveness, necrosis, hypoxia and gene expression[30–34]. We therefore hypothesized that significantly different values of PET image derived heterogeneity quantification featuresmay be

observed between the different BC molecular subgroups, assuming these subgroups have different underlying physiopathological properties.

Only few studies investigated ^{18}FDG-PET imaging heterogeneity features in BC [9,10]. A recent study investigated the relationship between ^{18}FDG heterogeneity quantification with TFs and histopathological factors, suggesting thatthe tumor heterogeneity measured on ^{18}FDG-PET/CT was higher in invasive BC with poor prognosis pathological factors, and that texture analysis might be used, in addition to SUV_{max}, as a new tool to assess invasive BC aggressiveness[9]. The combination of SUV_{max} with heterogeneity TFs indeed allowed the identification of the 13 TNBC cases among the 54 BC patients with an AUC of 0.83 instead of 0.77 when using SUV_{max} only, although this improvement was not significant[9]. The patient population was somewhat different from our study since it included 14 patients (26%) with distant metastases whilst we did not include patients with distant metastasis. Nonetheless, our results regarding SUV_{max} are congruent with data from this study and others [6,9]. On the other hand, our data suggest that none of the heterogeneity quantification metrics provided any added discriminative power in comparison with SUV_{max} regarding the differentiation of BC subgroups. We used the same 64 grey-level quantization and the same or similar TFs.

Another recent study investigated the heterogeneity of ^{18}FDG uptake in 123 BC patients, reporting on the prognostic value of MATV and heterogeneity, and found these two PET features to be associated with clinical outcome [10]. However in that study the “heterogeneity factor” (HF) used was defined as “a derivative of a volume threshold function from 40% to 80% of the SUV_{max}” and was reported to be highly correlated with MATV (r=0.96)[10]. On the one hand, HF was only a surrogate measurement of volume which led to the exact same survival curves. It cannot be

considered as a measurement of intra-tumor heterogeneity. On the other hand, we also included an alternative heterogeneity quantification metric (CH_{AUC}) [15], which similarly failed to exhibit any correlation with BC subgroups. The fact that textural analysis and the alternative CHAUC both failed to capture any correlation strengthens our overall conclusions.

In the present study, the correlation between MATV and its derived heterogeneity quantification ranged from 0.06 (for HILAE) to 0.88 (for D) depending on the metric, as previously shown [18,19]. Heterogeneity quantification may be more relevant and less correlated with the volume when it is calculated for large tumor volumes [19,21]. This is why we also performed a separate analysis on the 89 patients with volumes >10cm^3, a threshold value we have previously identified with respect to the correlation of MATV and TFs [19]. However, the results of this separate analysis were not different.

We evaluated the relationship betweenseveralPET-derived parameters and BC cancer subgroups based on immunohistochemical tests. The phenotype distribution in our series of 171 stage II-III BC patients (TNBC: 32%; HER2-positive: 19%; ER-positive/HER2-negative: 49%) was similar to other reports[35,36]. Our resultssuggest that the heterogeneity and variability, in terms of BC phenotype subgroups determined by immunohistochemistry, do not necessarily translate into measurable and significant differences in terms of heterogeneity features on ^{18}FDG-PET images. Conversely usual SUV metrics exhibit significant differences, with higher SUV_{max} uptake in TNBC than in ER-positive/HER2-negative and HER2-positive BC. However their discriminative power was limited, with substantial overlaps between the three subgroups (figure 3).Our results show that ^{18}FDG-

PET/CT does not provide quantitative measurements with enough discriminative power to replace biopsies and molecular analyses for BC subgroups classification.

The present results corroborate our previous findings that biological factors of poor prognosis such as hormone receptor negativity, TNBC, and high grade tumors have higher levels of ^{18}FDG uptake (SUV values) [6]. The relationship of these prognostic factors with image heterogeneity features is less clear-cut, although some correlation was observed, especially with hormone receptor expression (table 2).

Our study has some limitations. It is a retrospective analysis of prospectively collected patient data from a single institution.The involved lymph nodes were not included in the analysis, as only primary tumors were quantified, although the correlation between the various metrics quantifying heterogeneity in the primary tumors and the lymph node involvement was assessed. We used the FLAB algorithm to determine primary tumors' MATVs automatically. This algorithm optimized for PET imaging has demonstrated high accuracy, robustness and reproducibility in clinical practice. Although FLAB was used here as to include the entire heterogeneous uptake of the primary tumor, voxels with low SUV similar to the background level of uptake (such as necrosis areas) can be excluded from the volume of analysis used for heterogeneity quantification if this necrotic area is not in the center of the tumor volume, which is rare.

It should be emphasized that breast tumors could be affected by respiratory motion. TFs blurred out by respiratory motion in the reconstructed 3D static image, can be better resolved by 4D-PET imaging [37]. Combined with the limited spatial resolution of PET, this is a major limitation on the level of heterogeneity details that can be captured by any image analysis method. Although Time-Of-Flight (TOF) imaging may not significantly enhance the heterogeneity details in PET images since it

mostly enhances signal-to-noise ratio, not spatial resolution using a dedicated breast PET (Positron Emission Mammography) scanner could improve the evaluation of heterogeneity compared to standard PET/CT [38,39].

We chose to categorize patients into 3 subgroups (TNBC, HER2-positive and ER-positive/HER2-negative), which are based on immunohistochemistry tests and allow to define groups of patients with homogeneous treatments. Others categorizations could be considered: hormone positive breast tumors can be dichotomized into luminal A (ER-positive/HER2-negative, with low grade and low proliferation) and luminal B (which regroups high proliferative ER-positive/HER2-negative breast carcinoma and some ER-positive/HER2-positive tumors). This further dichotomization may alter our results, as recent studies suggested that luminal A tumorsare less ^{18}FDG-avid than luminal B [40]. Similarly to the extended analysis of lymph nodes heterogeneity quantification, this could be the subject of future investigations, although it is unlikely that the addition of another BC subgroup would allow to improve the PET features discriminative power.

Finally, the impact of heterogeneity metrics in other PET tracers might be of interest in BC [41] and should be further evaluated.

Conclusion

This study confirms the association between high values of SUV_{max} in BC primary tumor and some biological and immunohistochemical poor prognostic factors. In particular high-grade tumor exhibited higher ^{18}FDG uptake than low and intermediate grade. SUV_{max} was higher in the case of triple negative tumor than in the case of hormonal positive BC. In this series of stage II-IIIBC, tumor size had no significant

impact on ^{18}FDG uptake with similar SUV_{max} values in T3 tumors (>5cm) as in T2 tumors.

T3 tumors exhibited more heterogeneous ^{18}FDG uptake than T2 tumors, although overlaps were substantial (AUCs<0.75). Tumor grade was not found to be associated with volumetric metrics and limitedassociation was seen with regional heterogeneity. Estrogen and progesterone receptor expression were associated with several heterogeneity patterns, but the discriminative power was limited. Finally, the three different BC subgroups (ER-positive/HER2-negative, HER2-positive and TNBC) did not translate into any significant and measurable differences in the levels of heterogeneity.

Compliance with Ethical Standards

Funding: This work has received a French government support granted to the CominLabs excellence laboratory and managed by the National Research Agency in the "Investing for the Future" program under reference ANR-10-LABX-07-01.

Disclosure of Conflicts of Interest: The authors declare that they have no conflict of interest.

Research involving Human Participants and/or Animals: All procedures performed in studies involving human participants were in accordance with the ethical standards of the institutional and/or national research committee and with the 1964 Helsinki declaration and its later amendments or comparable ethical standards. For this retrospective study formal consent is not required.

REFERENCES

1. Groheux D, Hindié E, Delord M, Giacchetti S, Hamy A, de Bazelaire C, et al. Prognostic impact of (18)FDG-PET-CT findings in clinical stage III and IIB breast cancer. J. Natl. Cancer Inst. 2012;104:1879–87.

2. Cochet A, Dygai-Cochet I, Riedinger J-M, Humbert O, Berriolo-Riedinger A, Toubeau M, et al. ^{18}F-FDG PET/CT provides powerful prognostic stratification in the primary staging of large breast cancer when compared with conventional explorations. Eur. J. Nucl. Med. Mol. Imaging. 2014;41:428–37.

3. NCCN Clinical Practice Guidelines in Oncology. Breast Cancer. Version 3. 2014. Available at:http://www.nccn.org/professionals/physician_gls/f_guidelines.asp.

4. Groheux D, Giacchetti S, Espie M, Rubello D, Moretti JL, Hindie E. Early monitoring of response to neoadjuvant chemotherapy in breast cancer with 18F-FDG PET/CT: defining a clinical aim. Eur J Nucl Med Mol Imaging. 2011;38:419–25.

5. De Azambuja E, Holmes AP, Piccart-Gebhart M, Holmes E, Di Cosimo S, Swaby RF, et al. Lapatinib with trastuzumab for HER2-positive early breast cancer (NeoALTTO): survival outcomes of a randomised, open-label, multicentre, phase 3 trial and their association with pathological complete response. Lancet Oncol. 2014;15:1137–46.

6. Groheux D, Giacchetti S, Moretti JL, Porcher R, Espie M, Lehmann-Che J, et al. Correlation of high 18F-FDG uptake to clinical, pathological and biological prognostic factors in breast cancer. Eur J Nucl Med Mol Imaging. 2011;38:426–35.

7. Koolen BB, Vrancken Peeters MJTFD, Wesseling J, Lips EH, Vogel WV, Aukema TS, et al. Association of primary tumour FDG uptake with clinical, histopathological and molecular characteristics in breast cancer patients scheduled for neoadjuvant chemotherapy. Eur. J. Nucl. Med. Mol. Imaging. 2012;39:1830–8.

8. Oshida M, Uno K, Suzuki M, Nagashima T, Hashimoto H, Yagata H, et al. Predicting the prognoses of breast carcinoma patients with positron emission tomography using 2-deoxy-2-fluoro[18F]-D-glucose. Cancer. 1998;82:2227–34.

9. Soussan M, Orlhac F, Boubaya M, Zelek L, Ziol M, Eder V, et al. Relationship between tumor heterogeneity measured on FDG-PET/CT and pathological prognostic factors in invasive breast cancer. PloS One. 2014;9:e94017.

10. Son SH, Kim D-H, Hong CM, Kim C-Y, Jeong SY, Lee S-W, et al. Prognostic implication of intratumoral metabolic heterogeneity in invasive ductal carcinoma of the breast. BMC Cancer. 2014;14:585.

11. Wolff AC, Hammond MEH, Schwartz JN, Hagerty KL, Allred DC, Cote RJ, et al. American Society of Clinical Oncology/College of American Pathologists guideline recommendations for human epidermal growth factor receptor 2 testing in breast cancer. Arch. Pathol. Lab. Med. 2007;131:18–43.

12. Hatt M, Cheze le Rest C, Descourt P, Dekker A, De Ruysscher D, Oellers M, et al. Accurate automatic delineation of heterogeneous functional volumes in positron

emission tomography for oncology applications. Int J Radiat Oncol Biol Phys. 2010;77:301–8.

13. Hatt M, Cheze le Rest C, Turzo A, Roux C, Visvikis D. A fuzzy locally adaptive Bayesian segmentation approach for volume determination in PET. IEEE Trans Med Imaging. 2009;28:881–93.

14. Hatt M, Groheux D, Martineau A, Espié M, Hindié E, Giacchetti S, et al. Comparison between 18F-FDG PET image-derived indices for early prediction of response to neoadjuvant chemotherapy in breast cancer. J. Nucl. Med. Off. Publ. Soc. Nucl. Med. 2013;54:341–9.

15. Van Velden FH, Cheebsumon P, Yaqub M, Smit EF, Hoekstra OS, Lammertsma AA, et al. Evaluation of a cumulative SUV-volume histogram method for parameterizing heterogeneous intratumoural FDG uptake in non-small cell lung cancer PET studies. Eur J Nucl Med Mol Imaging. 2011;38:1636–47.

16. Tixier F, Le Rest CC, Hatt M, Albarghach N, Pradier O, Metges JP, et al. Intratumor heterogeneity characterized by textural features on baseline 18F-FDG PET images predicts response to concomitant radiochemotherapy in esophageal cancer. J Nucl Med. 2011;52:369–78.

17. Tixier F, Hatt M, Le Rest CC, Le Pogam A, Corcos L, Visvikis D. Reproducibility of tumor uptake heterogeneity characterization through textural feature analysis in 18F-FDG PET. J Nucl Med. 2012;53:693–700.

18. Hatt M, Tixier F, Cheze Le Rest C, Pradier O, Visvikis D. Robustness of intratumour ^{18}F-FDG PET uptake heterogeneity quantification for therapy response prediction in oesophageal carcinoma. Eur. J. Nucl. Med. Mol. Imaging. 2013;40:1662–71.

19. Hatt M, Majdoub M, Vallières M, Tixier F, Le Rest CC, Groheux D, et al. 18F-FDG PET Uptake Characterization Through Texture Analysis: Investigating the Complementary Nature of Heterogeneity and Functional Tumor Volume in a Multi-Cancer Site Patient Cohort. J. Nucl. Med. 2015;56:38–44.

20. Galavis PE, Hollensen C, Jallow N, Paliwal B, Jeraj R. Variability of textural features in FDG PET images due to different acquisition modes and reconstruction parameters. Acta Oncol. 2010;49:1012–6.

21. Brooks FJ, Grigsby PW. The effect of small tumor volumes on studies of intratumoral heterogeneity of tracer uptake. J Nucl Med. 2014;55:37–42.

22. Benjamini Y, Hochberg Y. Controlling the False Discovery Rate: A Practical and Powerful Approach to Multiple Testing. J R Stat. Soc B. 1995;57:289–300.

23. El Naqa I, Grigsby P, Apte A, Kidd E, Donnelly E, Khullar D, et al. Exploring feature-based approaches in PET images for predicting cancer treatment outcomes. Pattern Recognit. 2009;42:1162–71.

24. Aerts HJWL, Velazquez ER, Leijenaar RTH, Parmar C, Grossmann P, Cavalho S, et al. Decoding tumour phenotype by noninvasive imaging using a quantitative radiomics approach. Nat. Commun. 2014;5:4006.

25. Lambin P, Rios-Velazquez E, Leijenaar R, Carvalho S, van Stiphout RG, Granton P, et al. Radiomics: extracting more information from medical images using advanced feature analysis. Eur J Cancer. 2012;48:441–6.

26. Apostolova I, Steffen IG, Wedel F, Lougovski A, Marnitz S, Derlin T, et al. Asphericity of pretherapeutic tumour FDG uptake provides independent prognostic value in head-and-neck cancer. Eur. Radiol. 2014;24:2077–87.

27. Tixier F, Hatt M, Valla C, Fleury V, Lamour C, Ezzouhri S, et al. Visual Versus Quantitative Assessment of Intratumor 18F-FDG PET Uptake Heterogeneity: Prognostic Value in Non-Small Cell Lung Cancer. J. Nucl. Med. Off. Publ. Soc. Nucl. Med. 2014;55:1235–41.

28. Cook GJ, Yip C, Siddique M, Goh V, Chicklore S, Roy A, et al. Are pretreatment 18F-FDG PET tumor textural features in non-small cell lung cancer associated with response and survival after chemoradiotherapy? J Nucl Med. 2013;54:19–26.

29. Groheux D, Giacchetti S, Delord M, de Roquancourt A, Merlet P, Hamy AS, et al. Prognostic impact of 18F-FDG PET/CT staging and of pathological response to neoadjuvant chemotherapy in triple-negative breast cancer. Eur. J. Nucl. Med. Mol. Imaging. 2015;42:377–85.

30. Tixier F, Groves AM, Goh V, Hatt M, Ingrand P, Le Rest CC, et al. Correlation of intra-tumor 18F-FDG uptake heterogeneity indices with perfusion CT derived parameters in colorectal cancer. PloS One. 2014;9:e99567.

31. Basu S, Kwee TC, Gatenby R, Saboury B, Torigian DA, Alavi A. Evolving role of molecular imaging with PET in detecting and characterizing heterogeneity of cancer tissue at the primary and metastatic sites, a plausible explanation for failed attempts to cure malignant disorders. Eur J Nucl Med Mol Imaging. 2011;38:987–91.

32. Rajendran JG, Schwartz DL, O'Sullivan J, Peterson LM, Ng P, Scharnhorst J, et al. Tumor hypoxia imaging with [F-18] fluoromisonidazole positron emission tomography in head and neck cancer. Clin. Cancer Res. Off. J. Am. Assoc. Cancer Res. 2006;12:5435–41.

33. Kunkel M, Reichert TE, Benz P, Lehr H-A, Jeong J-H, Wieand S, et al. Overexpression of Glut-1 and increased glucose metabolism in tumors are associated with a poor prognosis in patients with oral squamous cell carcinoma. Cancer. 2003;97:1015–24.

34. Alvarez JV, Belka GK, Pan T-C, Chen C-C, Blankemeyer E, Alavi A, et al. Oncogene pathway activation in mammary tumors dictates FDG-PET uptake. Cancer Res. 2014;74:7583–98.

35. Straver ME, Rutgers EJ, Rodenhuis S, Linn SC, Loo CE, Wesseling J, et al. The relevance of breast cancer subtypes in the outcome of neoadjuvant chemotherapy. Ann Surg Oncol. 2010;17:2411–8.

36. Esserman LJ, Berry DA, DeMichele A, Carey L, Davis SE, Buxton M, et al. Pathologic complete response predicts recurrence-free survival more effectively by cancer subset: results from the I-SPY 1 TRIAL--CALGB 150007/150012, ACRIN 6657. J. Clin. Oncol. Off. J. Am. Soc. Clin. Oncol. 2012;30:3242–9.

37. Yip S, McCall K, Aristophanous M, Chen AB, Aerts HJWL, Berbeco R. Comparison of texture features derived from static and respiratory-gated PET images in non-small cell lung cancer. PloS One. 2014;9:e115510.

38. Koolen BB, Vidal-Sicart S, Benlloch Baviera JM, Valdés Olmos RA. Evaluating heterogeneity of primary tumor (18)F-FDG uptake in breast cancer with a dedicated breast PET (MAMMI): a feasibility study based on correlation with PET/CT. Nucl. Med. Commun. 2014;35:446–52.

39. Kalinyak JE, Berg WA, Schilling K, Madsen KS, Narayanan D, Tartar M. Breast cancer detection using high-resolution breast PET compared to whole-body PET or PET/CT. Eur. J. Nucl. Med. Mol. Imaging. 2014;41:260–75.

40. Humbert O, Berriolo-Riedinger A, Cochet A, Gauthier M, Charon-Barra C, Guiu S, et al. Prognostic relevance at 5 years of the early monitoring of neoadjuvant chemotherapy using (18)F-FDG PET in luminal HER2-negative breast cancer. Eur. J. Nucl. Med. Mol. Imaging. 2014;41:416–27.

41. Linden HM, Dehdashti F. Novel methods and tracers for breast cancer imaging. Semin. Nucl. Med. 2013;43:324–9.

	Number of patients (%) *N*=171
Tumor classification†	
T1	3(2)
T2	72(42)
T3	61(36)
T4	35(20)
Lymph node classification†	
N0	63(27)
N1	76(44)
N2	26(15)
N3	6(4)
Grade	
Grade-1	5(3)
Grade-2	75(44)
Grade-3	90(53)
Unspecified	1(<1)
Histological Type	
Invasive ductal, no special type	156(91)
Lobular	7(4)
Metaplastic	6(4)
Other	2(1)
ER	
Positive	95(56)
Negative	76(44)
PR	
Positive	57(33)
Negative	112(66)
Unspecified	2(1)
HER2	
Positive	33(19)
Negative	138(81)
BC Subgroup	
ER+/HER2-	84(49)
HER2+	33(19)
Triple Negative	54(32)

Table1.Patients and tumors characteristics

† Clinical classification before ^{18}FDG-PET/CT according to the 7th edition of the AJCC Staging Manual.

PET feature	ANOVA p-value [AUC of ROC curve]					
	Age >40 y *vs.* ≤40 y N=171	Age >50 y *vs.* ≤50 y N=171	T-score 1+2 *vs.* 3 N=136	N-score N0 *vs.* N1-3 N=171	Histology N=166	Tumor grade 1+2 *vs.* 3 N=170
SUV_{max}	0.588	0.096	0.809	0.411	0.034*	**<0.001 [0.779]**
SUV_{mean}	0.444	0.090	0.740	0.440	0.047*	**<0.001 [0.769]**
MATV	0.252	0.567	**<0.001 [0.740]**	0.137	0.531	0.034*
TLG	0.306	0.786	**<0.001 [0.670]**	0.405	0.406	**<0.001 [0.694]**
CH_{AUC}	0.480	0.673	**0.018 [0.617]**	0.162	0.943	0.052
D	0.746	0.707	**<0.001 [0.736]**	0.119	0.876	0.199
E	0.782	0.639	**<0.001 [0.652]**	0.851	0.989	0.040*
H	0.737	0.732	**<0.001 [0.730]**	0.052	0.691	0.227
HILAE	0.516	0.917	0.050*	0.365	0.686	**0.012 [0.624]**
ZP	0.964	0.482	**<0.001 [0.685]**	0.189	0.495	0.064

PET feature	ANOVA p-value [AUC of ROC curve]						
	ER N=171	PR N=169	HER2 N=171	BC subgroups			
				All patients (N=171)			MATV>10cm^3 (N=89)
				TNBC N=54	ER+/HER2- N=84	HER2+ N=33	
SUV_{max}	**<0.001 [0.672]**	**<0.001 [0.670]**	0.633	**<0.001 [0.713]**	**<0.001 [0.675]**	**[0.514]**	0.045*
SUV_{mean}	**<0.001 [0.658]**	**0.001 [0.653]**	0.422	**<0.001 [0.709]**	**<0.001 [0.651]**	**[0.547]**	0.033*
MATV	**0.015 [0.600]**	**0.024 [0.599]**	0.598	0.089			0.475
TLG	**<0.001 [0.658]**	**0.001 [0.650]**	0.489	**0.001 [0.669]**	**[0.637]**	**[0.516]**	0.339
CH_{AUC}	0.934	0.699	0.133	0.143			0.206
D	**0.009 [0.615]**	**0.019 [0.604]**	0.679	0.045*			0.475
E	0.099	**0.025 [0.600]**	0.403	0.070			0.063

H	**0.014 [0.607]**	**0.033 [0.599]**	0.286	0.090	0.478
HILAE	0.700	0.384	0.298	0.194	0.176
ZP	0.086	0.049	0.181	0.177	0.403

Table 2. Association between PET features and clinical, histological and immunohistochemical factors, with associated discriminative power [AUC of ROC curves] when significant

Significant results in **bold**.
* not significant after correction for multiple testing.

FIGURES

Fig. 1. FLAB delineation (green) in two tumors. Entropy values are expressed between 0 and 1. (Left) MATV = 25.5 cm^3, SUV_{max} = 10.4, Entropy = 0.89 (Right) MATV = 23.9 cm^3, SUV_{max} = 3.9, Entropy= 0.54.

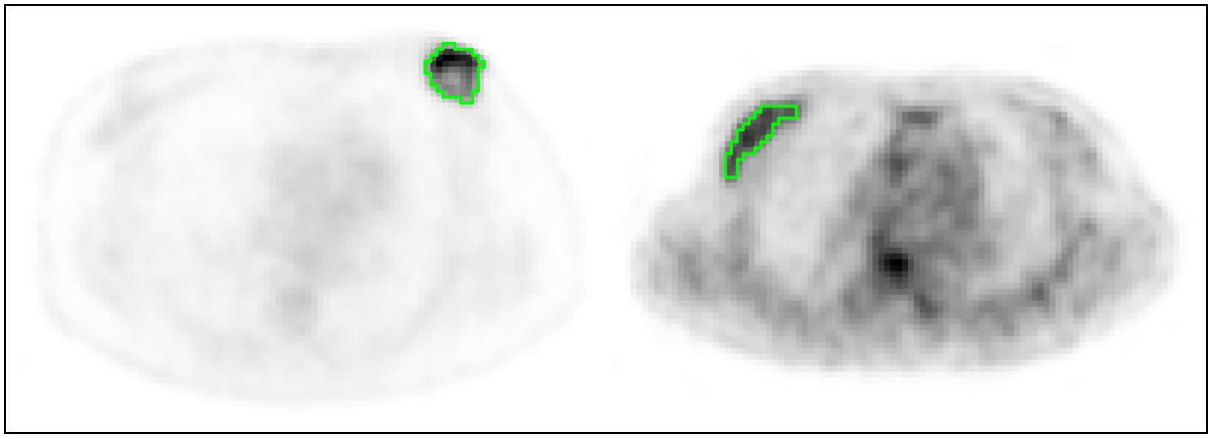

Fig.2. Distributions of SUV_{max} in grade 1-2 *vs.* grade 3 tumors.

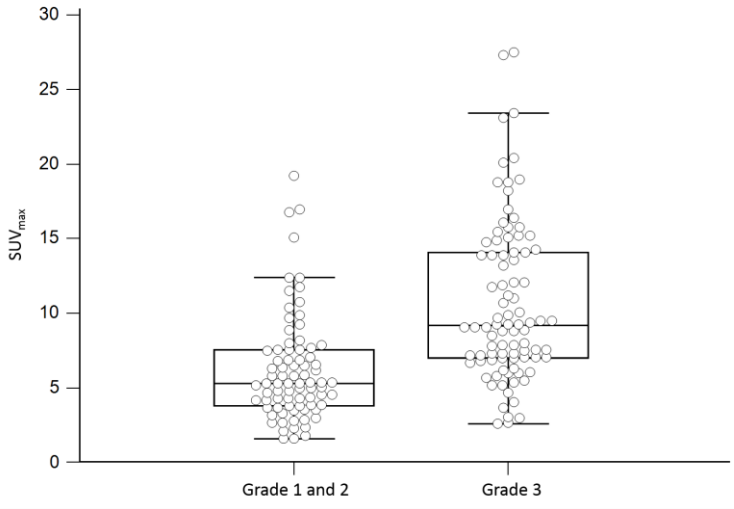

Fig.3. Distributions of (A) SUV_{max}, (B) MATV in the three subgroups.

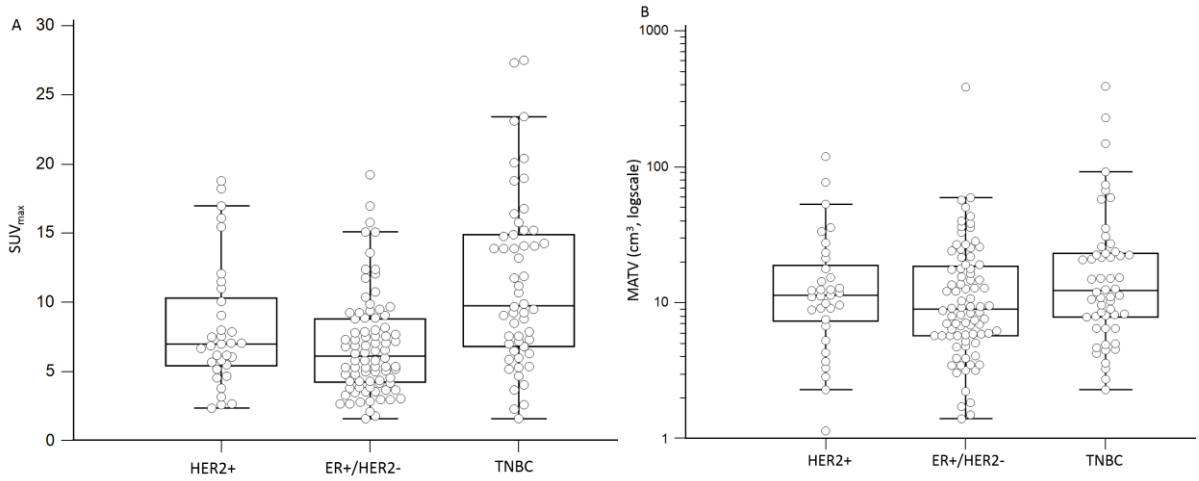

Fig.4. ROC curves for the differentiation of each subgroup using SUV_{max}: (A) HER2-positive, (B) ER-positive/HER2-negative and (C) TNBC.